

Frequency Dependency of Pacing Determinants of an IK1-mediated Rotor Drift in the Posterior Left Atrial Wall toward the Pulmonary Veins

Conrado J Calvo^{1,2,3}, Makarand Deo¹, Sharon Zlochiver^{1,4}, José Millet^{2,3}, Omer Berenfeld^{1,5}

¹Center for Arrhythmia Research, Department of Internal Medicine, University of Michigan, USA

²BioITACA Bioingeniería Instituto de Aplicaciones Avanzadas Universitat Politècnica de Valencia, Spain

³Departamento Ingeniería Electrónica. Universitat Politècnica de Valencia, Spain

⁴Department of Biomedical Engineering, Tel Aviv University, Israel

⁵Department of Biomedical Engineering, University of Michigan, USA

Abstract

Maintenance of paroxysmal atrial fibrillation (AF) by fast rotors near or at the pulmonary veins (PVs) is not fully understood. We believe that heterogeneous distribution of transmembrane currents in the PVs and LA junction (PV-LAJ) play a major role in the localization of rotors in the PVs. We seek for pacing protocols and measurements that could be used to predict drift direction. Experimentally observed heterogeneities in the PV-LAJ were incorporated into 2D and pseudo-3D models of Courtemanche-Ramirez-Nattel-Kneller human atrial kinetics to simulate various conditions and investigate rotor drifting mechanisms and electrophysiological pacing predictors. Simulations with various I_{K1} gradient conditions and various current-voltage relationships, substantiated its major role in the rotor drift. Among various action potential properties tested, only MDP gradient was found to be a pacing-rate independent predictor of rotor drift direction. Our simulations suggest that I_{K1} heterogeneity is dominant in conveying the drift direction through its impact on the global excitability and refractoriness gradients and more importantly it is only reflected in pacing studies in a frequency dependent manner. Our results call out for precaution when extrapolating results determined from pacing studies, commonly performed at 2 Hz.

1. Introduction

The mechanisms of atrial fibrillation (AF), the most common cardiac arrhythmia in the clinical practice, are not fully understood. Acute AF in normal isolated sheep hearts has been found to depend often on fast rotors localized mainly to the posterior wall of the left atrium (LA) and the pulmonary veins (PVs) junction (PV-LAJ) with fibrillatory conduction toward the rest of the atria.[1] Recent clinical data also points to rotors in various atrial

sites as a mechanism driving paroxysmal AF[2,3] and simulations of rotors in the PV-LAJ already demonstrated that they can occur under appropriate PV size and non-uniform coupling conditions.[4] However, both the time-course of the rotors in the PV-LAJ as well as the ionic properties that underlie the propensity of the rotors to be found in the PV area in some patients, but not in others, are yet to be investigated.

Previous studies on simplified cardiac models have linked rotor drift to spatial heterogeneity in the action potential properties.[5] Accordingly, rotors would drift toward regions with prolonged action potential duration (APD) or reduced excitability,[6] but since the ionic determinants of APD and excitability are numerous it is necessary to combine the effect of spatial dispersion in all currents to predict the rotor dynamics in the PV-LAJ. In particular, I_{K1} and I_{Kr} have been separately linked to rotor dynamics by affecting both the membrane APD and excitability in a similar manner,[7,8] and the PV-LAJ of the dog has been found to consist of non-uniform I_{K1} and I_{Kr} characterized by gradients in opposite directions,[9] precluding a simple prediction of the rotor dynamics.

Our study aims to elucidate ionic mechanisms and pacing predictors of rotor drifting at the PV-LAJ. We propose a set of measures to confirm our mechanistic proposition linking the ionic properties of the atrial substrate and the predisposition of the PVs, or any other region, to attract or reject rotor activity during AF.[10,11]

2. Methods

Numerical simulations were performed on 2- and pseudo 3-D structures of the area of transition between the LA and the PV. Both a 50×50 mm² regular 2D square model and a pseudo-3D cylindrical surface model were constructed by applying no-flux boundary conditions at the LA and PV edges and periodic boundary conditions on the other two edges of a regular 2D mesh. Heterogeneous ionic conditions were implemented

following a spatial Boltzmann distribution of conductance for I_{K1} , I_{Ks} , I_{Kr} , I_{to} , and I_{CaL} between the LA and the PV based on data from dogs [9].

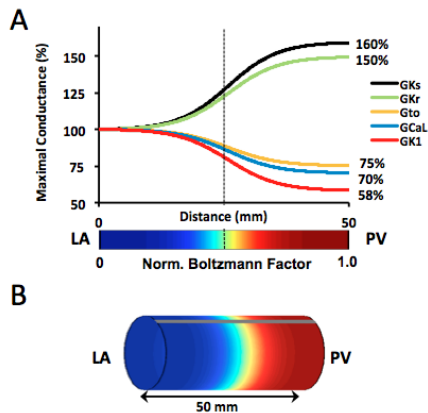


Figure 1. A. Spatial gradients included and model used.

3. Rotor characterization in homogeneous LA and PV models

The baseline relationship between the substrate and single rotor was studied in 2D models with homogeneous ionic conductances of the LA and PV, separately from each other. Rotors were initiated by cross-field stimulation protocol and then their spontaneous evolution was characterized. Tracking the pivoting point of the rotors by their respective PS reveals a meandering, without drift, in an area of diameters of about 11.4 mm. The LA rotor was slightly faster at 7.7 Hz in comparison with PV rotor at 7 Hz, which was consistent with larger space-time averaged sodium channels availability, $h \cdot j$, in the LA (0.38) than in the PV (0.29) [Table 1].

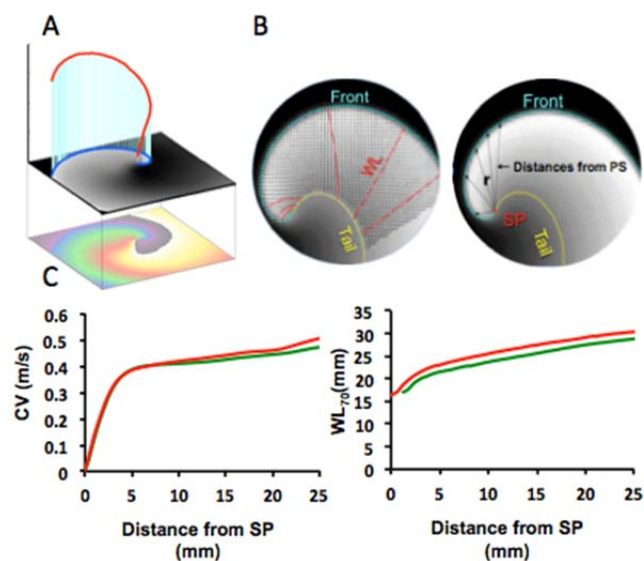


Figure 1. Rotor characterization. A. Correspondence between wave front and simulated voltage, where parameters were estimated. B. Diagrams showing parameters measured from rotors in each model. C. Spatial variation of CV and WL measured radially from the Singularity Point (SP).

Figure 1, Panels A and B, illustrate how the distance between the isopotential line of the front (blue) and the PS was determined and how the local CV vectors and the wavelength stretched between the isopotentials of the front (blue) and the tail (yellow). The bottom diagrams (Figure 2C) shows that overall, rotor properties as a function of the distance from its PS in the PV model showed slightly lower front curvature (not shown), conduction velocity (CV), action potential duration (not shown) and wavelength (WL₇₀) in comparison with the values in the LA model.

Table 1. Rotor Dynamics Characterization on LA and PV homogeneous models.

Parameter	LA	PV
Core diameter (mm)	11.5	11.3
Rotor Frequency (Hz)	7.7	7
Spatiotemporal $\langle h \cdot j \rangle$	0.38	0.29

4. Attraction of rotors at the PV-LAJ to the PVs

Our simulations showed rotor drift toward the PVs with IK1-mediated dominance with lower density at the PV than the LA (Figures 2,3). Despite gradients in I_{Kr} and I_{K1} were opposed [9] the latter was dominant conveying drift direction as shown in Figure 2,B.

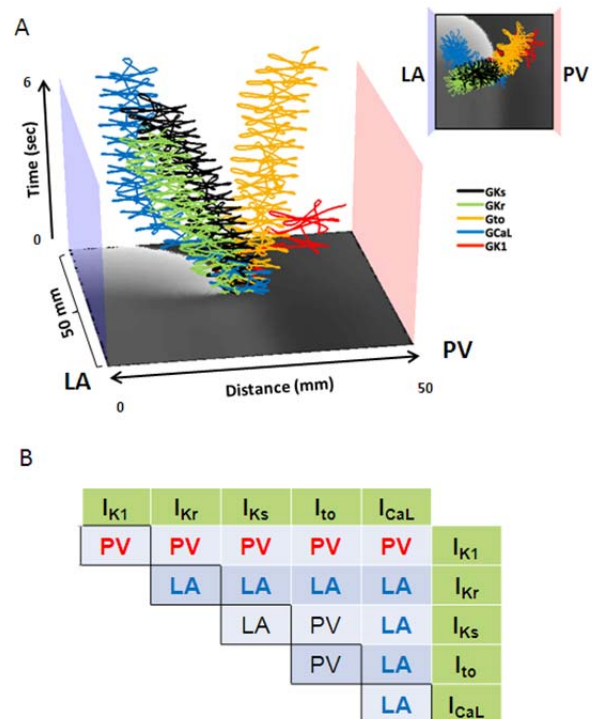


Figure 2. Reentry drift and individual/paired spatial gradients. A. Effect of spatial gradient of each individual current on reentry drift. B. Effect of spatial gradients in paired currents on reentry drift.

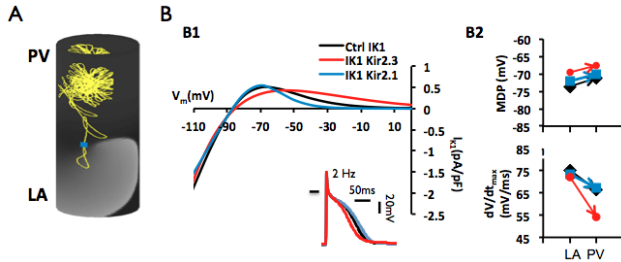


Figure 3. Rotor drift toward the PV-end, independently of the dominant isoform, was in good agreement with measured dV/dt_{max} and MDP. A. SP tracing of rotor drift on the pseudo-3D heterogeneous PVLAJ model. B. IK1 I-V curves tested in our simulations. C. 2s interval dV/dt_{max} and MDP measured at the LA and PV ends.

When all gradients were included independently of the dominant IK1 isoform drift direction was in good agreement with discrete gradient on upstroke velocity (dV/dt_{max}) and maximum diastolic potential (MDP) measured at the LA and PVs (Figure 3).

Finally, in the next illustration (Figure 4) we additionally demonstrate that that heterogeneity is required within the core region to induce rotor drift.

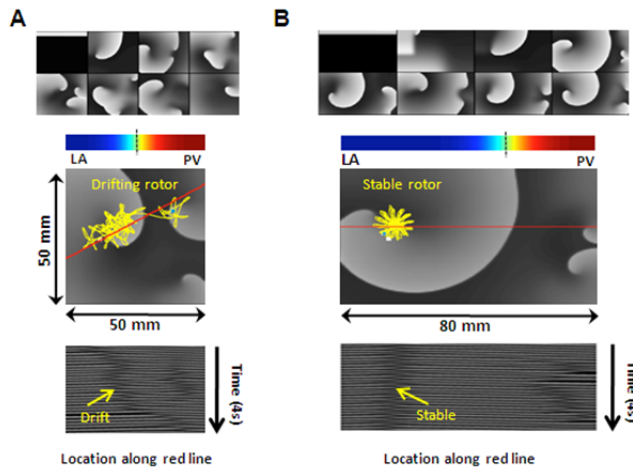


Figure 4. Ionic gradient at the vicinity of the core and rotor drift. A. Simulation in a $50 \times 50 \text{ mm}^2$ model of the PV-LAJ whose Boltzmann distribution is varying throughout the model. B. Simulation in a $80 \times 50 \text{ mm}^2$ model of the PV-LAJ whose Boltzmann distribution is mostly uniform in the LA portion of the model. Top panel show snapshots of activation in time. Middle panel show tracing of SP for the dominant rotor. Bottom panel represent V_m time-space plots across the red lines shown above.

5. Pacing predictors for drift direction

We sought for pacing protocols and measurements that could be used to predict drift direction. Our results showed that measures at 2Hz independently of the conditions simulated did not correlate well with drift direction. In Figure 5, we show APD profiles consequential of a steady pacing at the center of the

junction, where rotors were initiated previously, and use radial propagation at twice the threshold current for excitation. Panel A display distinct variation of duration at different repolarization levels during increasing pacing rate from 2 to 7 Hz; the bar-graph at the bottom compares APD values for 1000, 500 and 140 ms cycle length (respectively 1, 2 and 7.14 Hz pacing rates) and shows that while at 1 Hz pacing the PV APD is shorter than the LA at all repolarization levels, at 2 Hz and even more so at 7 Hz (close to the rotor frequency), APD_{90} at the PV edge is longer than in the LA. Panel D shows that APD_{80} , dV/dt_{max} and ERP across the model measured only at a cycle lengths of 140 ms (7.14 Hz) resulted in gradient directions consistent with the previous prediction of the drift toward longer APD and lower excitability [6].

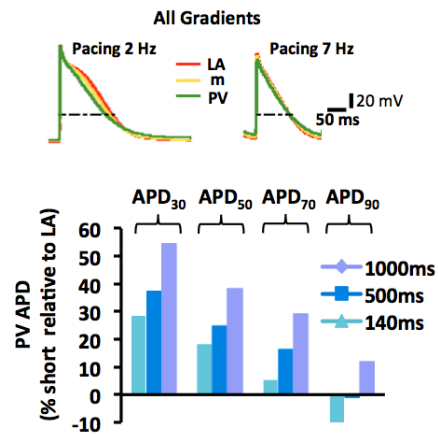


Figure 5. APD as traditional predictor of drift direction. APD below 70% of repolarization and measured and low frequencies is a bad predictor of substrate dependent predisposition for drift direction. Top panel show single pixel recordings at three locations across the PVLAJ: LA (red), middle (yellow) and PV (green) locations; during steady state pacing at 2Hz vs 7Hz. Bottom panel show APD quantification at different repolarization levels and stimulation frequencies. Notably, at all pacing rates slower than 140 ms, (7.14 Hz - close to the rotation frequencies in the LA and PV) the APD in the PV is shorter than in the LA (except APD_{90} at 140 and 500 ms).

As shown in the next illustration (Figure 6), measurements of APD, ERP and upstroke velocity revealed frequency dependent agreement with drift direction. At lower frequencies, 1 and 2Hz stimulation (commonly used in pacing studies), PV showed shorter APD and ERP as compared to LA. However this gradient was reversed at 7Hz, which is the resultant dominant frequency at which the tissue is activated when reentry is induced in the PVLAJ model.

Similar results were observed in the upstroke velocity measurements (during pacing). However, the LA-PV dispersion of MDP displayed a rate-independent correlation with the drift direction; regardless of the pacing rate, the drift was found consistently toward the region with the most positive MDP.

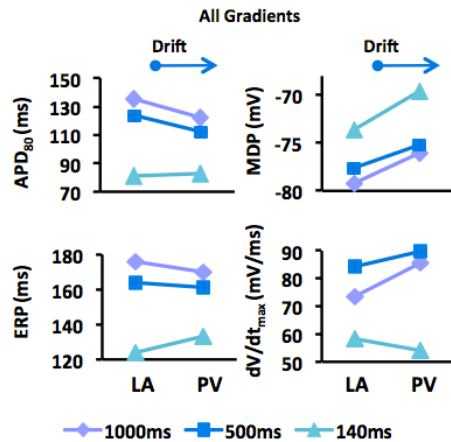


Figure 6. Frequency-dependence of parameter measure during steady-state constant pacing stimulation. Single Pixel APD_{80} , ERP, MDP and dV/dt_{max} in the LA and PV as measured at 1000 (diamond purple), 500 (square dark blue) and 140 ms (triangle light blue) pacing rate. Drift direction is also indicated (arrows on top).

6. Conclusions

Consistent with experimental and clinical studies on paroxysmal AF, our simulations in an ionically heterogeneous model of the PV-LAJ showed rotor attraction towards the PVs. Our simulations also suggest that regardless of a particular ionic dispersion of the PV-LAJ, measuring with high-resolution refractoriness, excitability and diastolic potentials during pacing could provide a mechanistic guidance for the unstable components of rotors that are believed to underlie AF.

These results provide a novel framework for the understanding of the complex dynamics of rotors in AF and gives insight on interpretation of frequency dependent electrophysiological measurements in the EP Lab.

Acknowledgements

None. Supported in part by: the Coulter Foundation from the Biomedical Engineering Department (University of Michigan); the Gelman Award from the Cardiovascular Division (University of Michigan); the National Heart, Lung, and Blood Institute grants (P01-HL039707 and P01-HL087226), and the Leducq Foundation.

References

[1] Mandapati R, Skanes A, Chen J, Berenfeld O, Jalife J. Stable microentrant sources as a mechanism of atrial fibrillation in the isolated sheep heart. *Circulation* 2000;18;101(2):194-9

[2] Atienza F, Almendral J, Moreno J, Vaidyanathan R, Talkachou A, Kalifa J, Arenal A, Villacastin JP, Torrecilla EG, Sanchez A, Ploutz-Snyder R, Jalife J, Berenfeld O. Activation of inward rectifier potassium channels accelerates atrial fibrillation in humans: evidence for a reentrant mechanism. *Circulation* 2006;114(23):2434-42.

[3] Narayan SM, Krummen DE, Shivkumar K, Clopton P, Rappel WJ, Miller JM. Treatment of atrial fibrillation by the ablation of localized sources: CONFIRM (Conventional ablation for atrial Fibrillation with or without focal Impulse and Rotor Modulation) Trial. *J Am Coll Cardiol* 2012;60(7):628-36.

[4] Cherry EM, Ehrlich JR, Nattel S, Fenton FH. Pulmonary vein reentry--properties and size matter: insights from a computational analysis. *Heart Rhythm* 2007;4(12):1553-62.

[5] Pertsov AM, Davidenko JM, Salomonsz R, Baxter WT, Jalife J. Spiral waves of excitation underlie reentrant activity in isolated cardiac muscle. *Circ Res* 1993;72(3):631-50.

[6] Fast VG, Pertsov AM. Drift of a vortex in the myocardium. *Biophysics* 1990;35:489-94.

[7] Campbell K, Calvo CJ, Mironov S, Herron T, Berenfeld O, Jalife J. Spatial gradients in action potential duration created by regional magnetofection of hERG are a substrate for wavebreak and turbulent propagation in cardiomyocyte monolayers. *J Physiol* 2012;590(Pt 24):6363-79.

[8] Noujaim SF, Pandit SV, Berenfeld O, Vikstrom K, Cerrone M, Mironov S, Zugermayr M, Lopatin AN, Jalife J. Up-regulation of the inward rectifier K⁺ current (I_{K1}) in the mouse heart accelerates and stabilizes rotors. *J Physiol* 2007;578(Pt 1):315-26.

[9] Ehrlich JR, Cha TJ, Zhang LM, Chartier D, Melnyk P, Hohnloser SH, Nattel S. Cellular electrophysiology of canine pulmonary vein cardiomyocytes: action potential and ionic current properties. *Journal of Physiology-London* 2003;551(3):801-13.

[10] Arora R, Verheule S, Scott L, Navarrete A, Katari V, Wilson E, Vaz D, Olgin JE. Arrhythmogenic substrate of the pulmonary veins assessed by high-resolution optical mapping. *Circulation* 2003;107(13):1816-21.

[11] Po SS, Li Y, Tang D, Liu H, Geng N, Jackman WM, Scherlag B, Lazzara R, Patterson E. Rapid and stable re-entry within the pulmonary vein as a mechanism initiating paroxysmal atrial fibrillation. *J Am Coll Cardiol* 2005;45(11):1871-7.

Address for correspondence.

Conrado J Calvo.
Bio-ITACA Universitat Politècnica de Valencia
Camí de Vera, s/n
46022 Valencia, Spain
conradca@itaca.upv.es